Geophysical Research Letters

RESEARCH LETTER
10.1029/2019GL082093

Sensitivity of Acoustic Emission Triggering to Small Pore Pressure Cycling Perturbations During Brittle Creep

K. Chanard[1,2], A. Nicolas[2], T. Hatano[3], F. Petrelis[4], S. Latour[5], S. Vinciguerra[6], and A. Schubnel[2]

[1]Université de Paris, Institut de physique du globe de Paris, CNRS, IGN, Paris, France, [2]Laboratoire de Géologie, CNRS UMR 8538, École normale Supérieure, PSL Research University, Paris, France, [3]Earthquake Research Institute, University of Tokyo, Tokyo, Japan, [4]Laboratoire de Physique Statistique, École Normale Supérieure, PSL Research University, Paris, France, [5]IRAP, Université Paul Sabatier, Toulouse, France, [6]Department of Earth Sciences, University of Turin, Turin, Italy

Key Points:
- We investigate the role of periodic pore fluid pressure on AEs triggering during creep deformation experiments
- AEs correlation with pore pressure oscillations increases as the rock approaches failure
- AEs occur significantly more when pore pressure decreases, that is, when deformation is maximum

Supporting Information:
- Supporting Information S1
- Data Set S1

Correspondence to:
K. Chanard,
chanard@ipgp.fr

Citation:
Chanard, K., Nicolas, A., Hatano, T., Petrelis, F., Latour, S., Vinciguerra, S., & Schubnel, A. (2019). Sensitivity of acoustic emission triggering to small pore pressure cycling perturbations during brittle creep. *Geophysical Research Letters*, *46*. https://doi.org/10.1029/2019GL082093

Received 16 JAN 2019
Accepted 17 JUN 2019
Accepted article online 1 JUL 2019

Abstract Fluid-induced stress perturbations in the crust at seismogenic depths caused by sources such as tidal or seasonal loading may trigger earthquakes. We investigate the role of small periodic pore pressure (P_p) perturbation in rupture nucleation by performing laboratory triaxial creep experiments on Fontainebleau sandstone, saturated in water, under sinusoidal P_p variations. Results show that recorded acoustic emissions (AEs) correlate with P_p as the rock approaches failure. More interestingly, AEs occur significantly more when P_p is decreasing, that is, when strain rate is maximum with a progressive increase of P_p-AEs correlation in time as the rock approaches failure. This suggests that the correlation of small stress perturbations and AEs not only depends on P_p amplitude but also on the criticality of the rock. Observations at the laboratory scale support field observations where tidal loading may have modulated seismic rates during the nucleation phase of the 2004 Sumatra-Andaman and 2011 Tohoku-Oki earthquakes.

1. Introduction

While regional stresses may remain below the frictional strength of faults for periods of decades to centuries, fluid-induced transient stress perturbations may initiate significant slip on a fault. In the Earth's crust, at seismogenic depths, transient changes in stress can be caused by various sources, and their role in earthquake triggering is key to a better understanding of the seismic cycle. Among them, fluid sources have attracted much interest over the past decades such as (1) anthropogenic activities (reservoir-filling, fluid injection, or withdrawal; Amos et al., 2014; McGarr et al., 2002; Talwani, 1998; van der Elst et al., 2013), (2) solid Earth tides and ocean loading (Cochran et al., 2004; Ide & Tanaka, 2014; Métivier et al., 2009. Tanaka et al., 2002, 2004; Thomas et al., 2012), (3) deglaciation unloading (Dahl-Jensen et al., 2010; Sauber & Molnia, 2004), (4) seasonal variations in continental water storage (Ader & Avouac, 2013; Bollinger et al., 2007; Bettinelli et al., 2008; Christiansen et al., 2005; Craig et al., 2017; Johnson et al., 2017; Heki, 2003), and (5) magmatic fluid pressurizations and volcanic unrest (Chouet, 1996; Fazio et al., 2017; Hill et al., 2002; Manga & Brodsky, 2006; McNutt, 1996; Savage & Cockerham, 1984)

Mechanisms involved in slip initiation on faults by short-term small stress variations, as well as the time evolution of a fault strength under such conditions, are poorly understood. Particularly, the role of periodic stress perturbations (tidal loading and seasonal continental water variations) in triggering or modulating efficiently seismicity remains a debated question (Vidale et al., 1998).

Interestingly, Dieterich (1992) proposed that short-period stress transients are not effective at triggering earthquakes if they occur faster than nucleation times. Lockner and Beeler (1999) estimated an earthquake nucleation time close to a year by scaling results from stick slip rock mechanics experiments, where granite samples were periodically deformed in a triaxial apparatus. Later on, the authors used this estimate to explain the poor correlation between tidal loading and earthquakes (Beeler & Lockner, 2003). However, several robust studies showed a statistically significant correlation between Earth and Moon tides and earthquakes (Cochran et al., 2004; Ide & Tanaka, 2014; Métivier et al., 2009; Rydelek et al., 1988; Thomas et al., 2012) and even at higher frequencies between dynamic triggering from seismic waves and earthquakes

(Hill & Prejean, 2007). In addition to the loading frequency and amplitude of transient periodic perturbations, the state of stress of a fault may play an important role in its sensitivity to short-term small stress variations as suggested by the observation of an increase in correlation between tidal loading and seismicity localized in nucleation zones of large earthquakes: the Sumatra megathrust earthquakes of 26 December 2004 (M_w 9.0), 28 March 2005 (M_w 8.6), and 12 September 2007 (M_w 8.5; Tanaka, 2010), and the 2011 Tohoku-Oki earthquake (M_w 9.1; Tanaka, 2012). Faults in a critical state should be sensitive to small stress perturbations that may contribute, when added to a high preexisting stress, to failure, and, on the contrary, faults far from failure would be insensitive to small periodic loading. In order to address this issue, we deform Fontainebleau sandstone samples in the laboratory. Rock samples are loaded at constant stress in brittle creep conditions (or static fatigue in the engineering literature) to simulate tectonic loading, combined with small sinusoidal pore pressure (Pp) variations of controlled amplitudes, analogous to tides or seasonal loading. Our experimental setup aims at testing the influence of small periodic stress perturbations on shear fracture nucleation at in situ pressure conditions. In particular, we monitor the triggering of acoustic emissions (AEs) that precedes shear failure of brittle rock samples, as a function of the amplitude of periodic stress perturbation and the general stress state of the rock under brittle creep deformation. In section 2, we describe the sample preparation and experimental setup used in our study. In section 3, we present experimental observations of deformation and AEs occurrence from both constant strain rate and pore pressure stress-cycling experiments with various amplitudes and the associated AEs records. Finally, in section 4, we discuss experimental results and their potential implications on large-scale field observations.

2. Experimental Setup and Testing Conditions

2.1. Material and Sample Preparation

Samples used in this study are part of a single block of Fontainebleau sandstone (France), formed of pure quartz grains that are well sorted and have a nearly uniform grain size of around 250 μm (Bourbie & Zinszner, 1985), isotropic, with 7% porosity. Cylindrical samples are cored in the block, with a diameter of 40 mm and a mean length of 86 mm, end-polished with a 5-μm precision to assure parallel cuts, and dried. We glued two pairs of strain gauges (radial and axial) on opposite sides of the sample (supporting information Figure S1a). Rock samples are then placed in a neoprene jacked to ensure impermeability to confining oil. Jackets are drilled to glue 16 acoustic sensors directly on the sample's surface (supporting information Figure S1b). Acoustic sensors are piezoceramic transducers (PZTs) made of a piezoelectric crystal sensitive to P waves (normal to the sample-sensor surface), mounted on a brass holder. Once the sensors are glued, a soft glue around the PZTs ensures the jacket impermeability. PZTs are distributed on five lines, with two to five sensors (supporting information Figure S1c). Finally, the sample is placed dried inside the pressure vessel and then saturated in the apparatus. More information about this experimental setup can be found in Brantut et al. (2011).

2.2. Experimental Setup

We run experiments in an externally heated triaxial cell which uses oil as the pressure medium located at the École Normale Supérieure (Brantut et al., 2011). Volumetric servo-pumps control the confining pressure P_c, measured by a pressure transducer with an accuracy of 1 kPa. The axial stress is controlled by an independent piston and volumetric servo-pump (up to 680 MPa on a 40-mm diameter sample).

Axial deformation of rock samples is measured by averaging three eddy current sensors fixed at the bottom end of the cell, with a precision of 0.3 μm. Deformation measurements are corrected for the deformation of the apparatus itself. All our experiments are run at a controlled temperature of 35 °C using the external heating system surrounding the vessel, consisting in a silicone heated sleeve around the vessel. The temperature is recorded with two thermocouples.

We use a double microvolumetric pump to impose a pore pressure within the sample. The pump is made of two separate pistons, running together or independently. During our experiments, the two pumps are connected to the two entrance points of the pore fluid pressure network. Either the pumps receive fluid that is discharged by the system or, if the pore pressure decreases, they inject fluid into the sample. We record pore pressure variations within the sample using a sensor located at its bottom. We also use pumps to control oscillations of pore pressure using an automated schedule of injecting and receiving fluid of the two pumps.

Acoustic sensors in the vessel are connected to the outside by 16 high-voltage coaxial wires, plugged into high-frequency 40-dB amplifiers with two distinct outputs. A trigger logic insures that signals above a certain

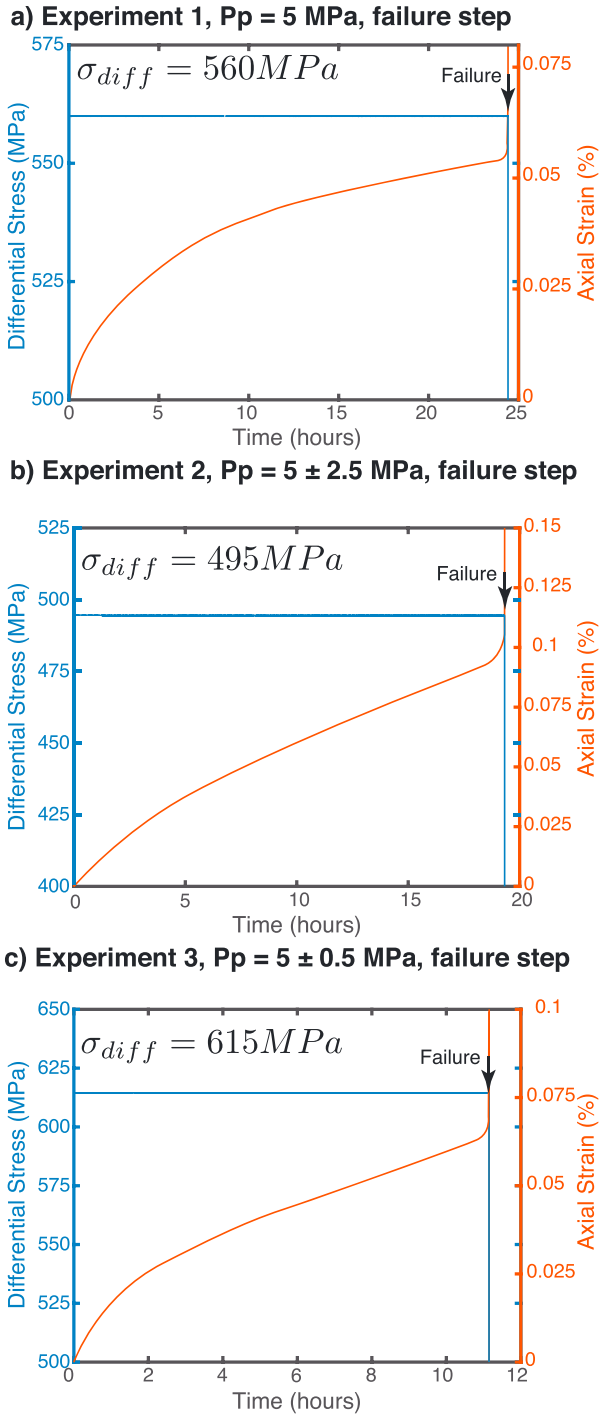

Figure 1. Differential stress (blue) and axial strain (red) as a function of elapsed time during the last differential stress step prior to failure for (a) Experiment 1, where the pore pressure is constant at 5 MPa, and (b) Experiment 2 and (c) Experiment 3 where the pore pressure is a periodic function with period T_p = 244 s and amplitude of 5±2.5 and 5±0.5 MPa, respectively.

threshold amplitude on a given number of channels are recorded on the oscilloscopes at 50-MHz sampling rate. In our case, to ensure catalog completeness, the trigger logic was set relatively high (three channels above 300 mV during a 5-ms window).

Local strains are measured using two pairs of strain gauges (axial and radial). Stresses and strains are recorded at 1-Hz frequency through a dedicated interface. In addition, global axial strains are determined by measuring the total displacement of the piston.

2.3. Experimental Conditions

We deform rock samples under brittle creep conditions, that is, under a long-term constant stress, below the short-term failure stress of the material, by increasing axial stress by steps (supporting information Figure S2), and under constant or oscillating pore pressure. All experiments were conducted at a regulated temperature of 35 °C and a constant 35-MPa confining pressure.

For bulk rock deforming under brittle creep conditions, deformation is a nonlinear function of time (Main, 2000; Main et al., 1993) exhibiting a bimodal behavior in a time-axial strain plane. The function exhibits a two-stage creep curve likely representing the product of a decelerating creep phase followed by an accelerating creep phase until rock failure (Figure 1). This deformation mode has been largely experimentally observed (Baud & Meredith, 1997; Brantut et al., 2013; Lockner, 1993; Main, 2000).

In addition to classical brittle creep conditions, we run experiments under controlled pore pressure conditions: Experiment 1 is realized as a reference under a constant pore pressure of 5 MPa, Experiment 2 with an oscillating pore pressure at 5±2.5 MPa, and Experiment 3 under oscillating pore pressure at 5±0.5 MPa, both with a loading period of $T_p = 244$ s. Note that the three rock samples from a single Fontainebleau sandstone block failed at significantly different differential stresses, most likely due to heterogeneities within the block, but at similar deformation rates (Figure 1). In these experiments, the characteristic hydraulic diffusion time is $t_{hy} = \frac{L^2\eta}{k*K_\phi}$, where L is the characteristic diffusion length (assumed equal to the sample's length, i.e., 0.08 m), η the fluid dynamic viscosity ($\eta = 1 \times 10^{-3}$ Pa s), k the permeability (in square meters) and $K_\phi = \frac{1}{\frac{\phi}{K_f} + \frac{1-\phi}{K_s}}$ (in Pascals) is a poroelastic effective bulk modulus, where K_f and K_s are respectively the fluid ($K_f = 2 \times 10^9$ Pa) and solid matrix bulk moduli ($K_s = 40 \times 10^{10}$ Pa) and ϕ the porosity ($\phi = 0.07$). Because the permeability of our Fontainebleau sandstone is of the order of $k \sim 1 \times 10^{-16}$ m^2 (Bourbie & Zinszner, 1985; David et al., 2013), the characteristic diffusion timescale is of the order of a couple of seconds, that is, much lower than the pore pressure cycling period of $T_p = 244$ s. Hence, we can consider that at all times, the pore pressure is at equilibrium within the specimen.

3. Experimental Results: AEs

We present results from three experiments in which rock samples were loaded by the combined action of constant stress (creep), intended to simulate tectonic loading, and a constant or small sinusoidal pore pressure oscillation of various amplitudes, analogous to tides or seasonal loading. For each experiment, we record a catalog of AEs in order to investigate the correlation of pore pressure oscillations with acoustic activity. In addition, we provide insights on the temporal evolution of the correlation between pore pressure oscillations and acoustic activity prior to sample failure.

3.1. Correlation Between Pore Pressure Oscillations and AEs

We investigate the possible correlation between the occurrence of AEs and pore pressure oscillations, during the constant differential stress prior to brittle failure, when most of the AEs are recorded. We stack the AEs over a single pore pressure cycle with a period of $T_p = 244$ s for each experiment. As expected, AEs (gray) visually appear to occur randomly when stacked over T_p in Experiment 1, where the pore pressure is maintained constant and equal to 5 MPa (red) (Figure 2a). In Experiments 2 and 3 (Figures 2b and 2c), where the pore pressure oscillates with a period of T_p and amplitude of 5±2.5 and 5±0.5 MPa, respectively, the AEs occur significantly more when the pore pressure is decreasing (Figures 2b and 2c). We conclude that the pore pressure oscillation, even with a low amplitude, modulates AEs triggering prior to sample failure.

To statistically detect all potential periodic events, we perform a Schuster spectrum over the constant differential stress step of failure by computing a spectrum of Schuster p values independently over a range of

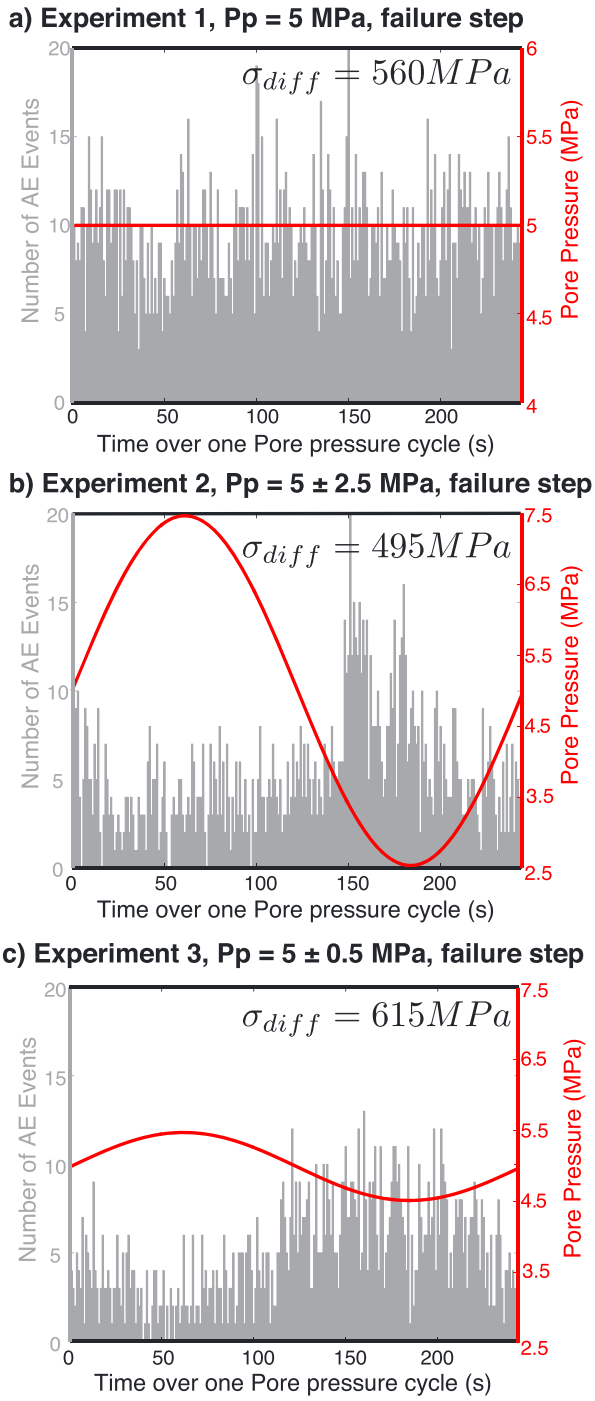

Figure 2. Coherent mean over the differential stress step of brittle failure for (a) Experiment 1, (b) Experiment 2, and (c) Experiment 3 of AEs (gray) and pore pressure oscillations (red) over a stacked cycle of pore pressure oscillation. AE = acoustic emission.

frequencies, including the pore pressure oscillation period (Ader & Avouac, 2013). The Schuster test determines a probability p value of the null hypothesis that the relative times of events can be achieved by a uniform random process assuming each sample is independent (Schuster, 1897). The Schuster p value is defined as

$$p = e^{-L^2/N} \tag{1}$$

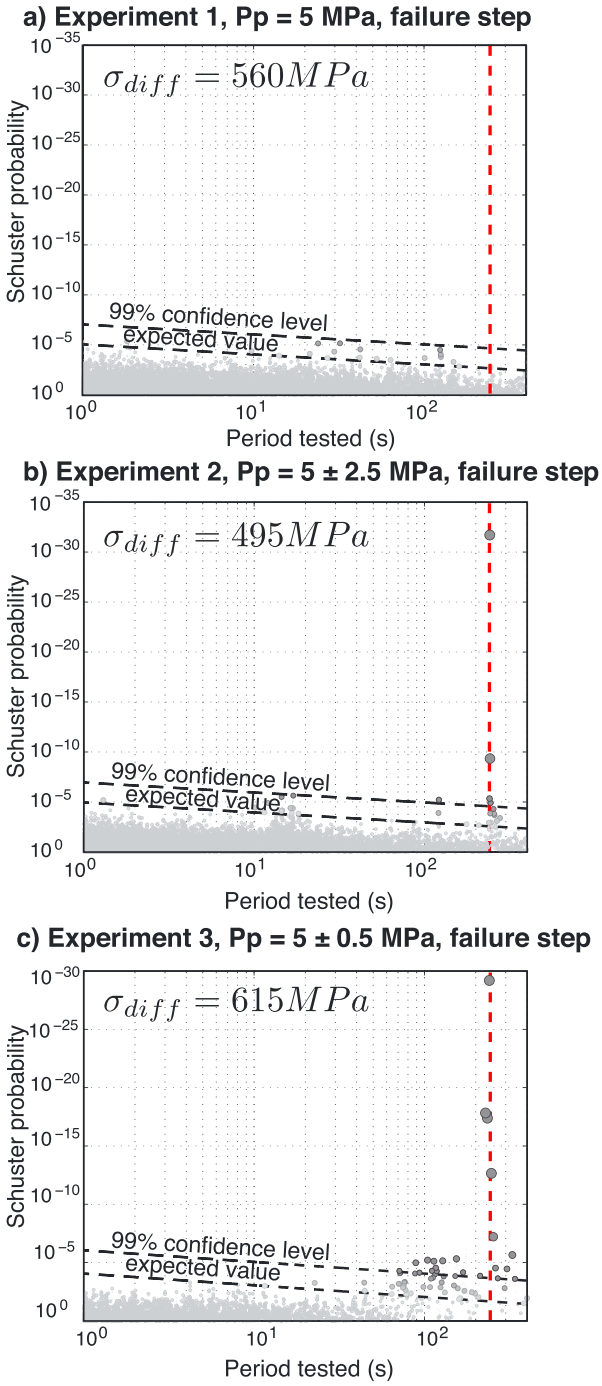

Figure 3. Schuster spectrum computed for Acoustic Emission (AE) catalogs of (a) Experiment 1, where the pore pressure is constant at 5 MPa, and (b) Experiment 2 and (c) Experiment 3 where the pore pressure is a periodic function with period T_p = 244 s and amplitude of 5±2.5 and 5±0.5 MPa, respectively. Period T is indicated in red and the expected Schuster probability value p asserting the existence of a periodicity and its 99% confidence level. Note that size of symbols for each period tested is inversely proportional to the logarithm of Schuster p value. For example, the larger the symbol, the higher the probability of an existing periodicity in the AEs catalog.

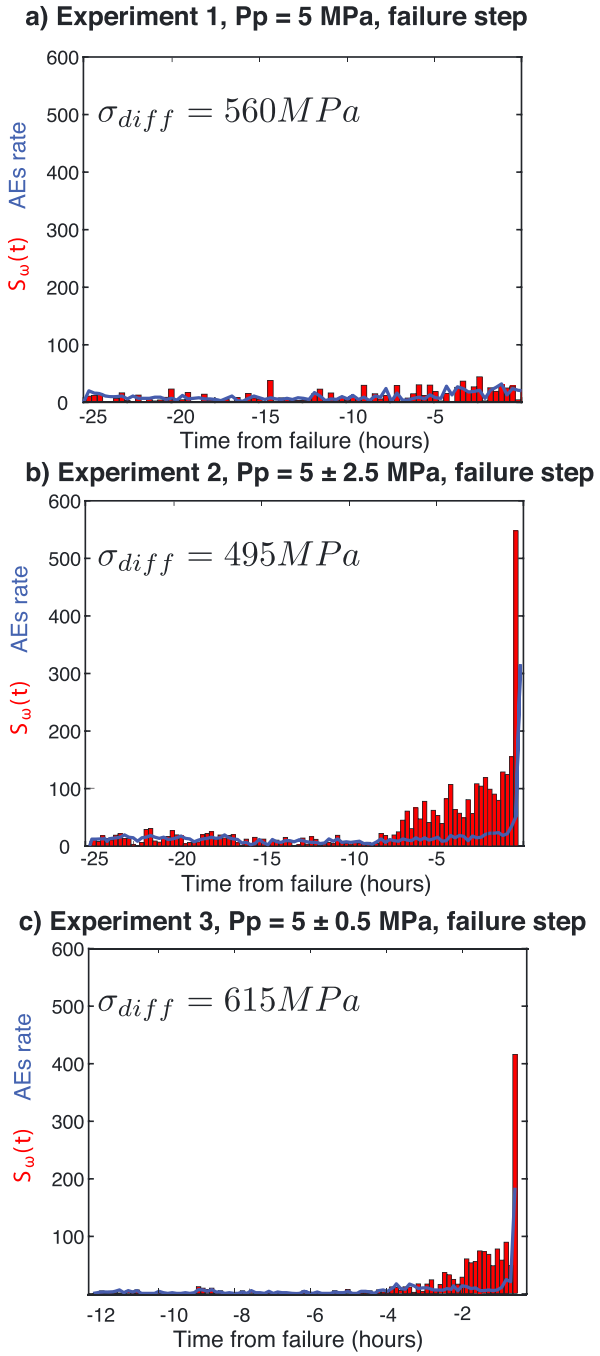

Figure 4. Time evolution of the correlation between Acoustic Emission (AE) events occurring during the differential stress step of failure and the pore pressure oscillations of pulsation $\omega=2\pi/T_p$, $T_p = 244$ s, for Experiment 1 (a), Experiment 2 (b), and Experiment 3 (c). AEs rates are shown in blue. For both experiments with pore pressure oscillations, the correlation coefficient increases progressively during a few hours before rupture, with no significant increase of the AEs rate.

where N is the number of AEs in a time interval duration T, and L is the distance between the initial point to the final point of a random walk, which is defined as

$$L^2 = \left(\sum_{i=1}^{N} \cos(2\pi \frac{t_i}{T})\right)^2 + \left(\sum_{i=1}^{N} \sin(2\pi \frac{t_i}{T})\right)^2 \quad (2)$$

t_i is the time of the ith AE event and T is the period being considered. A small p value indicates that the probability of a random process is low and that the distribution is nonuniform, which is interpreted as evidence of periodicity. A periodicity in the AEs catalog will have a significant probability not to be due to chance if its Schuster p value is significantly lower than the expected value for a nonperiodic process (we choose the 99% confidence level as described by Ader & Avouac, 2013). By applying the Schuster test to AEs catalogs over a range of independent frequencies, the resulting Schuster spectrum can detect multiple periodicities, if any in the experiments, and help to identify the role of clustering effects in the catalog that might influence the correlation observed in Figure 2 between pore pressure oscillations and AEs occurrence (Ader & Avouac, 2013).

Figure 3 shows the results of the Schuster spectrum test for each experiment. The Schuster probability of the AEs catalogs is shown as a function of the period tested. For experiments 2 and 3, the pore pressure is a periodic function of period $T_p = 244$ s; the Schuster probability of observing the same periodicity in the AEs catalog exceeds the 99% confidence level. As expected, Experiment 1, where the pore pressure remains constant, shows no particular periodicity in the catalog of AEs.

From Figures 2 and 3, we conclude that when rock samples in brittle creep conditions experience pore pressure oscillations of period T, the AEs catalogs exhibit a statistically significant periodicity of same period T and that AEs occur preferentially when the pore pressure is decreasing.

3.2. Temporal Evolution of the Correlation Between Pore Pressure Oscillations and AEs

In order to follow the time evolution of AEs and pore pressure oscillations over the failure step, we describe the time evolution of Fourier components at the pore pressure oscillation frequency. For a number N of events occurring over a time step $[t, t+T_p]$, the correlation coefficient S_ω between pore pressure oscillations at a pulsation $\omega = \frac{2\pi}{T_p}$, where T_p is the cyclic loading period, and AEs is given by

$$S_\omega(t) = \left(\sum_{j=1}^{N} \cos(\omega t_j)\right)^2 + \left(\sum_{j=1}^{N} \sin(\omega t_j)\right)^2 \quad (3)$$

Figure 4 shows the time evolution of S_ω and of the AEs rate during the differential stress step of failure for (a) Experiment 1 where $Pp = 5$ MPa, (b) Experiment 2 where $Pp = 5\pm2.5$ MPa and (c) Experiment 3 where $Pp = 5\pm0.5$ MPa. Note that we removed the few seconds prior to rupture from the AEs catalog prior in all experiments due to the extremely large number of events occurring in a very short period and, hence, artificially correlating with the pressure oscillations. There is no significant increase in the correlation coefficient in the hours prior to rupture for Experiment 1. For Experiments 2 and 3, S_ω increases progressively during the 10 and 4 hr prior to rupture, respectively, with no significant increase of the AEs rates. This suggests that dynamic triggering or modulation of AEs by low-amplitude periodic pore pressure increases as the rock approaches failure, that is, during the rupture nucleation phase.

4. Discussion

We conducted laboratory experiments on Fontainebleau sandstone under constant stress, with superimposed sinusoidal pore pressure perturbations. Our experimental results show that (1) AEs and pore pressure oscillations are correlated, with more AEs occurring when the pore pressure is decreasing, and (2) the correlation coefficient between AEs and pore pressure oscillations progressively increases in time as the rock approaches brittle failure.

4.1. AEs Occurrence Controlled by Sample Deformation

From Mohr-Coulomb theory, one should expect that AEs occur preferentially when the pore pressure is maximum, in direct contradiction with our observation. A possible explanation as to why AEs statistically occur preferentially when the pore pressure is low is that the AE rate is correlated with strain rate rather than the maximum of pore pressure. The correlation between AE rate and strain rate has been ubiquitously observed during creep experiments on brittle rock (Brantut et al., 2013).

The macroscopic strain rate $\dot{\varepsilon}$ within samples in Experiments 2 and 3 is the combination of an inelastic creep strain rate $\dot{\varepsilon}_c$ term, due to subcritical microcrack propagation, and a poroelastic strain rate term $\dot{\varepsilon}_p$ as $\dot{\varepsilon}_T = \dot{\varepsilon}_c + \dot{\varepsilon}_p$. Strain rates $\dot{\varepsilon}$ estimated from the axial strain curves (Figure 1) are typically of the order

of magnitude of 10^{-8} s^{-1} (supporting information Figure S2) during the last creep stage prior to sample failure. The poroelastic strain rate can be estimated as well, from the following relation $\dot{\varepsilon}_p \sim -\delta P/(\Delta T K)$, where K is the bulk modulus of the rock sample, ΔP is the pore pressure perturbation, and ΔT is the period of oscillation. With pore pressure perturbations of ± 2.5 and ± 0.5 MPa over a 240-s period, $\dot{\varepsilon}_p$ is larger in amplitude than $\dot{\varepsilon}_c$ (using a typical bulk modulus of $K \sim 30$ GPa). In consequence, the macroscopic strain rate is negative when the pore pressure increases (poro-elastic unloading) and becomes positive only when the pore pressure starts decreasing. As a consequence, we observe more AEs when pore pressure decreases (Figure 2).

4.2. Relevance for Natural Earthquakes

The Earth's lithosphere constantly undergoes deformation induced by tectonic and nontectonic sources (redistribution in continental hydrology, oceanic or solid Earth tides, thermal forcing, etc.). Deformation occurs at timescales from subannual to millennial, with spatial scales ranging from a few kilometers to thousands of kilometers, and produces measurable geodetic signals. When regional deformation rates are small, possibly in plate interiors, where they are often close to the measurement precision, or in plate boundary regions during interseismic loading, both slow tectonic deformation and nontectonic sources can control the regional earthquakes rate. Our experimental creep conditions, where the sample is placed under creep deformation modulated or not by pore pressure oscillations, are analogous to a slowly deforming Earth's crust, possibly responding to periodic small nontectonic loading. Results from our experiments may give insights on the mechanisms modulating earthquakes, for which AEs are a proxy.

Ide (2013) showed that relative plate velocity in subduction zones, that is, the amount of deformation at plate boundaries, correlates with the occurrence of earthquakes in the region. This is coherent with observation (1) and the associated creep deformation model, where AEs are correlated with decreasing pore pressure, for example, with maximum deformation rate of the sample. Observation (2) suggests that the correlation of small stress perturbations and AEs increases with time as the rock approaches failure. This observation supports larger-scale observations of the increase in correlation between the earthquakes and tidal loading over a 10-year period prior to the Sumatra megathrust earthquakes of 26 December 2004 (M_w 9.0), 28 March 2005 (M_w 8.6), and 12 September 2007 (M_w 8.5; Tanaka, 2010) and the 2011 Tohoku-Oki earthquake (M_w 9.1; Tanaka, 2012). This suggests the statistical observation of modulation of earthquakes by periodic forcing could possibly provide useful information on the state of stress of a fault.

5. Conclusions

We presented results from creep experiments on Fontainebleau sandstone with periodic modulation of the sample pore pressure with different amplitudes. Our experiments suggest that transient stress perturbations play an important role in the modulation of AEs prior to rock failure in brittle creep experiments. Particularly, we show that pore pressure and AEs are correlated with the sample deformation rate and that the correlation coefficient between AEs and pore pressure oscillations progressively increases with time as the rock approaches failure.

The experimental results presented agree with observations at a larger scale, with earthquake rates correlating with deformation rates at plate boundaries (Ide, 2013), periodic modulation of earthquakes due to deformation induced by tidal or hydrological loading (Craig et al., 2017; Métivier et al., 2009), or increase in earthquakes-tidal loading correlation prior to large seismic events (Tanaka, 2010, 2012).

Further experiments will be needed to quantitatively investigate the relative contributions of the amplitude and frequency of the stress perturbation versus that of the driving force (strain rate).

Acknowledgments
This work was funded by the Laboratoire de Recherche Commun "Yves Rocard" (ENS-CEA-CNRS) and the ERC Realism (2016-grant 681346). This is IPGP contribution number 4042. Data supporting this study were obtained with the help of Yves Pinquier, using the triaxial cell at the École Normale Supérieure (Paris, France) and are available as supporting information. We thank the Editor and Associate Editor as well as two anonymous reviewers for their assistance in evaluating this paper.

References

Ader, T. J., & Avouac, J.-P. (2013). Detecting periodicities and declustering in earthquake catalogs using the Schuster spectrum, application to Himalayan seismicity. *Earth and Planetary Science Letters*, *377*, 97–105.

Amos, C. B., Audet, P., Hammond, W. C., Bürgmann, R., Johanson, I. A., & Blewitt, G. (2014). Uplift and seismicity driven by groundwater depletion in central California. *Nature*, *509*, 483–486.

Baud, P., & Meredith, P. (1997). Damage accumulation during triaxial creep of Darley Dale sandstone from pore volumometry and acoustic emission. *International Journal of Rock Mechanics and Mining Sciences*, *34*(3), 24–e1.

Beeler, N., & Lockner, D. (2003). Why earthquakes correlate weakly with the solid Earth tides: Effects of periodic stress on the rate and probability of earthquake occurrence. *Journal of Geophysical Research*, *108*(B8), 2391. https://doi.org/10.1029/2001JB001518

Bettinelli, P., Avouac, J. P., Flouzat, M., Bollinger, L., Ramillien, G., Rajaure, S., & Sapkota, S. (2008). Seasonal variations of seismicity and geodetic strain in the Himalaya induced by surface hydrology. *Earth and Planetary Science Letters*, *266*, 332–344.

Bollinger, L., Perrier, F., Avouac, J., Sapkota, S., Gautam, U., & Tiwari, D. (2007). Seasonal modulation of seismicity in the Himalaya of Nepal. *Geophysical Research Letters*, *34*, L08304. https://doi.org/10.1029/2006GL029192

Bourbie, T., & Zinszner, B. (1985). Hydraulic and acoustic properties as a function of porosity in Fontainebleau sandstone. *Journal of Geophysical Research*, *90*(B13), 11,524–11,532.

Brantut, N., Heap, M., Meredith, P., & Baud, P. (2013). Time-dependent cracking and brittle creep in crustal rocks: A review. *Journal of Structural Geology*, *52*, 17–43.

Brantut, N., Schubnel, A., & Guéguen, Y. (2011). Damage and rupture dynamics at the brittle-ductile transition: The case of gypsum. *Journal of Geophysical Research*, *116*, B01404. https://doi.org/10.1029/2010JB007675

Chouet, B. A. (1996). Long-period volcano seismicity: Its source and use in eruption forecasting. *Nature*, *380*(6572), 309.

Christiansen, L., Hurwitz, S., Saar, M., Ingebritsen, S., & Hsieh, P. (2005). Seasonal seismicity at western United States volcanic centers. *Earth and Planetary Science Letters*, *240*(2), 307–321.

Cochran, E. S., Vidale, J. E., & Tanaka, S. (2004). Earth tides can trigger shallow thrust fault earthquakes. *Science*, *306*(5699), 1164–1166.

Craig, T. J., Chanard, K., & Calais, E. (2017). Hydrologically-driven crustal stresses and seismicity in the New Madrid seismic zone. *Nature communications*, *8*(1), 2143.

Dahl-Jensen, T., Larsen, T. B., Voss, P. H., & Greenland Ice Sheet. (2010). Greenland Ice Sheet Monitoring Network (glisn): A seismological approach. *Geological Survey of Denmark and Greenland Bulletin*, *20*, 55–58.

David, E. C., Fortin, J., Schubnel, A., Guéguen, Y., & Zimmerman, R. W. (2013). Laboratory measurements of low-and high-frequency elastic moduli in Fontainebleau sandstone. *Geophysics*, *78*(5), D369–D379.

Dieterich, J. H. (1992). Earthquake nucleation on faults with rate-and state-dependent strength. *Tectonophysics*, *211*(1), 115–134.

Fazio, M., Benson, P. M., & Vinciguerra, S. (2017). On the generation mechanisms of fluid-driven seismic signals related to volcano-tectonics. *Geophysical Research Letters*, *44*, 734–742. https://doi.org/10.1002/2016GL070919

Heki, K. (2003). Snow load and seasonal variation of earthquake occurrence in Japan. *Earth and Planetary Science Letters*, *207*, 159–164.

Hill, D. P., Pollitz, F., & Newhall, C. (2002). Earthquake-volcano interactions. *Physics Today*, *55*(11), 41–47.

Hill, D., & Prejean, S. (2007). Dynamic triggering. *Treatise on Geophysics*, *4*, 257–292.

Ide, S. (2013). The proportionality between relative plate velocity and seismicity in subduction zones. *Nature Geoscience*, *6*(9), 780.

Ide, S., & Tanaka, Y. (2014). Controls on plate motion by oscillating tidal stress: Evidence from deep tremors in western Japan. *Geophysical Research Letters*, *41*, 3842–3850. https://doi.org/10.1002/2014GL060035

Johnson, C. W., Fu, Y., & Bürgmann, R. (2017). Seasonal water storage, stress modulation, and California seismicity. *Science*, *356*(6343), 1161–1164.

Lockner, D. (1993). Room temperature creep in saturated granite. *Journal of Geophysical Research*, *98*(B1), 475–487.

Lockner, D. A., & Beeler, N. M. (1999). Premonitory slip and tidal triggering of earthquakes. *Journal of Geophysical Research*, *104*(B9), 20,133–20,151.

Main, I. G. (2000). A damage mechanics model for power-law creep and earthquake aftershock and foreshock sequences. *Geophysical Journal International*, *142*(1), 151–161.

Main, I. G., Sammonds, P. R., & Meredith, P. G. (1993). Application of a modified griffith criterion to the evolution of fractal damage during compressional rock failure. *Geophysical Journal International*, *115*(2), 367–380.

Manga, M., & Brodsky, E. (2006). Seismic triggering of eruptions in the far field: Volcanoes and geysers. *Annual Review of Earth and Planetary Sciences*, *34*, 263–291.

McGarr, A., Simpson, D., & Seeber, L. (2002). Case histories of induced and triggered seismicity. *International Geophysics Series*, *81*(A), 647–664.

McNutt, S. R. (1996). Seismic monitoring and eruption forecasting of volcanoes: A review of the state-of-the-art and case histories, *Monitoring and mitigation of volcano hazards* (pp. 99–146). Berlin, Heidelberg: Springer.

Métivier, L., de Viron, O., Conrad, C. P., Renault, S., Diament, M., & Patau, G. (2009). Evidence of earthquake triggering by the solid Earth tides. *Earth and Planetary Science Letters*, *278*(3), 370–375.

Rydelek, P. A., Davis, P. M., & Koyanagi, R. Y. (1988). Tidal triggering of earthquake swarms at Kilauea volcano, Hawaii. *Journal of Geophysical Research*, *93*(B5), 4401–4411.

Sauber, J. M., & Molnia, B. F. (2004). Glacier ice mass fluctuations and fault instability in tectonically active southern Alaska. *Global and Planetary Change*, *42*(1), 279–293.

Savage, J., & Cockerham, R. (1984). Earthquake swarm in Long Valley Caldera, California, January 1983: Evidence for dike inflation. *Journal of Geophysical Research*, *89*(B10), 8315–8324.

Schuster, A. (1897). On lunar and solar periodicities of earthquakes. *Proceedings of the Royal Society of London*, *61*(369-377), 455–465.

Talwani, P. (1998). On the nature of reservoir-induced seismicity, *Seismicity associated with mines, reservoirs and fluid injections* pp. 473–492). Birkhäuser Basel: Springer.

Tanaka, S. (2010). Tidal triggering of earthquakes precursory to the recent Sumatra megathrust earthquakes of 26 December 2004 (M_w 9.0), 28 March 2005 (M_w 8.6), and 12 September 2007 (M_w 8.5). *Geophysical Research Letters*, *37*, L02301. https://doi.org/10.1029/2009GL041581

Tanaka, S. (2012). Tidal triggering of earthquakes prior to the 2011 Tohoku-Oki earthquake (m_w 9.1). *Geophysical Research Letters*, *39*, L00G26. https://doi.org/10.1029/2012GL051179

Tanaka, S., Ohtake, M., & Sato, H. (2002). Evidence for tidal triggering of earthquakes as revealed from statistical analysis of global data. *Journal of Geophysical Research*, *107*(B10), 2211. https://doi.org/10.1029/2001JB001577

Tanaka, S., Ohtake, M., & Sato, H. (2004). Tidal triggering of earthquakes in Japan related to the regional tectonic stress. *Earth, planets and space*, *56*(5), 511–515.

Thomas, A., Bürgmann, R, Shelly, D., Beeler, N., & Rudolph, M. (2012). Tidal triggering of low frequency earthquakes near Parkfield, California: Implications for fault mechanics within the brittle-ductile transition. *Journal of Geophysical Research*, *117*, B05301. https://doi.org/10.1029/2011JB009036

van der Elst, N. J., Savage, H. M., Keranen, K. M., & Abers, G. A. (2013). Enhanced remote earthquake triggering at fluid-injection sites in the midwestern United States. *Science*, *341*(6142), 164–167.

Vidale, J. E., Agnew, D. C., Johnston, M. J., & Oppenheimer, D. H. (1998). Absence of earthquake correlation with Earth tides: An indication of high preseismic fault stress rate. *Journal of Geophysical Research*, *103*(B10), 24,567–24,572.